Mechanisms of Strong-Field Double Ionization of Xe

Xufei Sun,[1] Min Li,[1,2] Difa Ye,[3] Guoguo Xin,[4] Libin Fu,[3,5,*] Xiguo Xie,[1] Yongkai Deng,[1] Chengyin Wu,[1,2] Jie Liu,[3,5] Qihuang Gong,[1,2] and Yunquan Liu[1,2,†]

[1]*Department of Physics and State Key Laboratory for Mesoscopic Physics, Peking University, Beijing 100871, China*
[2]*Collaborative Innovation Center of Quantum Matter, Beijing 100871, China*
[3]*Institute of Applied Physics and Computational Mathematics, 100088 Beijing, China*
[4]*Department of Physics, Northwest University, 710069 Xi'an, China*
[5]*HEDPS, Center for Applied Physics and Technology, Peking University, Beijing 100084, China*

(Received 8 July 2014; published 4 September 2014; corrected 9 September 2014)

We perform a fully differential measurement on strong-field double ionization of Xe by 25 fs, 790 nm laser pulses in intensity region $(0.4–3) \times 10^{14}$ W/cm^2. We observe that the two-dimensional correlation momentum spectra along the laser polarization direction show a nonstructured distribution for double ionization of Xe when decreasing the laser intensity from 3×10^{14} to 4×10^{13} W/cm^2. The electron correlation behavior is remarkably different with the low-Z rare gases, i.e., He, Ne, and Ar. We find that the electron energy cutoffs increase from $2.9U_p$ to $7.8U_p$ when decreasing the laser intensities from the sequential double ionization to the nonsequential double ionization regime. The experimental observation indicates that multiple rescatterings play an important role for the generation of high energy photoelectrons. We have further studied the shielding effect on the strong-field double ionization of high-Z atoms.

DOI: 10.1103/PhysRevLett.113.103001 PACS numbers: 32.80.Rm, 32.80.Fb, 32.90.+a, 42.50.Hz

Since the observation of the enhanced double ionization of He atoms at a moderate laser intensity, much attention has been concentrated on exploring the physical mechanism of nonsequential double ionization (NSDI) of atoms in strong laser fields [1]. Focusing on NSDI, now the generally accepted mechanism is provided by the strong-field three-step recollision model [2]: (i) the outer electron tunnels through the suppressed Coulomb barrier near the maximum laser field, (ii) it propagates in the strong infrared laser field, and (iii) it returns to the core to kick out the other inner electron remaining in the singly charged ion at the near zero crossing of the laser field with the maximum energy of $3.17U_p$ ($U_p = E_0^2/4\omega^2$, electron cycle-averaged quiver energy; E_0, field amplitude; ω, field frequency). Thus, the direct signatures of recollision in an $(e, 2e)$-like process are that the momentum distribution of the doubly charged ion shows the pronounced "double-hump" structure and both electrons are exclusively emitted into the same hemisphere along the polarization direction. Both have been observed in several experiments for low-Z rare gases, i.e., He, Ne, and Ar atoms [3–6]. It can be explained within the picture of recollision-induced direct ionization (RIDI).

Recent theoretical and experimental efforts have made much progress on NSDI of atoms (see for a review [7]). By decreasing the laser intensity below the recollision threshold, the striking back-to-back (anticorrelated) emission for Ar was observed [8], which was not able to be explained with the above simple RIDI picture. In this case, the energy of the recolliding electron up to $3.17U_p$ was below the field-modified ionization potential or even much less than the potential of the first excitation state of a singly charged ion [8,9]. Several other mechanisms, i.e., multiple recollisions [10] and recollision-induced excitation tunneling [11,12], have been implemented to explain the back-to-back correlation.

We should note that NSDI cannot be considered to be completely understood. Fully differential studies so far have been concentrated just on He, Ne, and Ar atoms. Until now, there has been no fully differential measurement on strong-field double ionization on high-Z atomic rare gases. If dating back the history of NSDI, the "knee" structure on the curve of the doubly charged ion yields vs laser intensity was first observed on Xe atoms [13]. Based on the measurements, several models, e.g., direct two-electron ejection [1], a high-order sequential mechanism [14], and a shake-off process during tunneling [15], were proposed. By measuring the photoelectron angular distribution of single ionization of Xe with the intensity dependence of the yields of double ionization, it was found that the nonresonant ionization process plays a role in the formation of doubly charged xenon ions [16]. By using the electron-ion coincident time-of-flight technique [17], the similarity of electron spectra from single ionization and double ionization of Xe was observed, which was attributed to the field-independent resonant excitation process [18]. Including the rescattering effect, the resonant model was subsequently invoked to explain the wavelength and intensity dependence of strong-field double ionization of Xe [19,20]. However, a major question about electron correlation dynamics itself for Xe has not been explored. This is the most direct approach toward distinguishing the mechanisms of NSDI and thus learning about their characteristics and production process.

In this Letter, we present a fully differential measurement on strong-field double ionization of Xe atoms in near-infrared fields over a wide range of laser intensities (4×10^{13}–3×10^{14} W/cm^2). Several striking observations characterize this case when decreasing the laser intensity from sequential double ionization (SDI) to NSDI of Xe: (i) the momentum distributions of doubly charged ions always show a single peak distribution (Gaussian-like); (ii) the characteristic correlation momentum spectra of NSDI, i.e., "side-by-side emission" [6] or "back-to-back emission" [9], essentially disappear; (iii) the electron energy cutoffs of double ionization increase from $2.9U_p$ to $7.8U_p$, decreasing the laser intensity from SDI to NSDI. The findings show that multiple rescatterings and electron mutual interaction in the final states contribute to the enhancement of double ionization of Xe atoms. Using the semiclassical two-electron atomic ensemble model, we have studied the electron shielding effect on strong-field ionization of high-Z atoms.

We used a linearly polarized Ti:sapphire amplified laser at 790 nm wavelength in 25 fs with a repetition rate of 3 kHz. The laser pulse was focused into the vacuum chamber of a cold-target recoil-ion-momentum spectroscopy [21] with a pressure better than 5×10^{-11} mbar. The fragmented ions and electrons were guided into two position-sensitive channel plate detectors by electric (~3 V/cm) and magnetic (~8 G) fields applied along the time-of-flight axis. From the time of flight and position on the detections, the full momentum vectors of coincident electrons and ions were calculated. The laser polarization direction was along the time-of-flight axis. Finally, we have the electron momentum resolution ~0.02 a.u. along the time-of-flight direction and ~0.05 a.u. along the transverse direction.

There are nine stable Xe isotopes with close mass numbers that can be resolved in the experiment. In order to measure the electron correlation spectra, it is very necessary to resolve all doubly charged isotopes in the coincidence with their electrons for the double ionization events (the estimated ratio of false coincidence events is ~8%–15%). In the off-line analysis, we did not select the double ionization events of ^{129}Xe and ^{132}Xe with a higher relative abundance because there are several isotopes with close atomic mass between them. It is hard to completely resolve the double ionization of those isotopes. We analyzed the coincident events of double ionization ^{134}Xe (relative abundance ~10.4%), and thus it took much time to obtain electron correlation spectra. In order to achieve reasonable statistics, we ran the measurement over weeks over a wide laser intensity scanning to achieve more than 10^5 double coincidence events (one $^{134}Xe^{2+}$ and one electron) for each laser intensity.

In order to calibrate the laser intensity, we first measured the momentum distributions of $^{40}Ar^{2+}$, as shown in Fig. 1(a). In the case of Ar, the momentum distribution exhibits the characteristic double-hump structure at an intensity of 3×10^{14} W/cm^2. The ubiquitous signature of RIDI is the occurrence of the prominent double-hump structure of Ar^{2+}. Dynamically, the electrons can gain the most probable longitudinal drift momentum $P^{\max}_{\parallel} = 2U_P{}^{1/2}$ (energy $E = 2U_p$) when they are created exactly at a zero crossing of the field, which is at the instance where the most energetic recollision occurs. Because of the typical recollision kinematics, this value of $P^{\max}_{\parallel}$ gives an upper classical limit for the most probable momenta of the doubly charged ion. Taking the perspective of the two electrons, both are left in the continuum after the recollision, collecting large drift momenta and emerging into the same hemisphere along the laser polarization direction. The final momentum of the doubly charged ion is thus balanced by the sum of all electron momenta, i.e., $4U_P{}^{1/2}$ [as indicated with arrows in Fig. 1(a)]. Along this line, the laser intensity can be calibrated [22].

To doubly check the precision of the laser intensity calibration, we have also measured the ratio of $^{134}Xe^{2+}/^{134}Xe^{+}$ (open circles), as shown in Fig. 1(c). Compared with the previous measurements on the ratio of integrated yields of Xe^{2+}/Xe^{+} (without identification of isotopes) with respect to the laser intensity (dotted curve) [18], the laser intensity agrees very well with the calibration using the momentum distribution of doubly charged ions. The calculated ratio of the ionization rate of Xe^{2+} and Xe^{+}

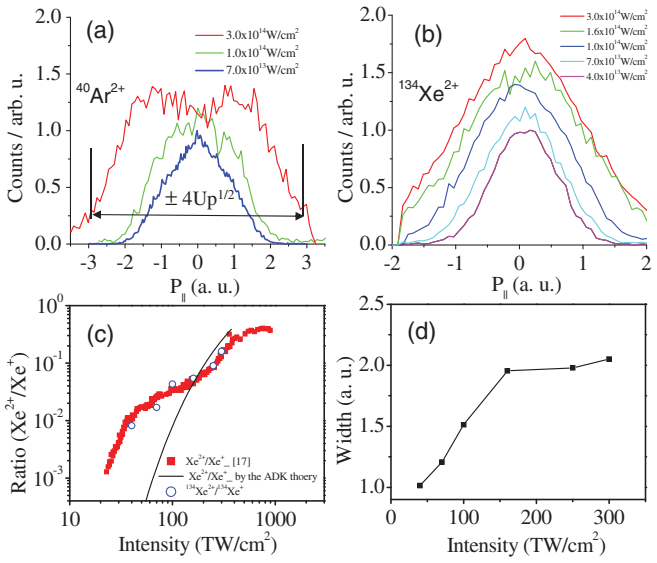

FIG. 1 (color). The longitudinal momentum distributions of (a) $^{40}Ar^{2+}$ and (b) $^{134}Xe^{2+}$ at intensities of $(0.4–3) \times 10^{14}$ W/cm^2 (25 fs, 790 nm). (c) The ratio of double to single ionization counts as a function of laser intensity for Xe. The dotted curve is taken from Ref. [17], where the isotopes are not resolved. The data marked with open circles are measured with $^{134}Xe^{2+}/^{134}Xe^{+}$ in this experiment. The solid line is the ratio of the Xe^{2+}/Xe^{+} ionization rate that is calculated by the ADK model. (d) The width (FWHM) of the longitudinal momentum distribution of Xe^{2+} with respect to the laser intensity.

with the Ammosov-Delone-Krainov (ADK) model [23] is also illustrated in Fig. 2(a) (solid curve). One can observe evidently the "knee" structure that is the signature of ionization enhancement. Such a comparison indicates that our experiment has really covered the SDI and NSDI regimes for Xe in strong laser fields.

In Fig. 1(b), we present the longitudinal momentum distributions of $^{134}Xe^{2+}$ decreasing from 3×10^{14} to 4×10^{13} W/cm^2. As seen in Fig. 1(d), the width (FWHM) of the momentum distributions increases with the laser intensity, and it will be saturated above the intensity of 2×10^{14} W/cm^2. Interestingly, the longitudinal momentum distributions of $^{134}Xe^{2+}$ do not reveal the typical double-hump structure in the NSDI regime, and they always show the Gaussian-like distribution with the maximum at zero momentum over a wide range of laser intensities. This feature is similar to the longitudinal momenta of Ar^{2+} below the recollision threshold, i.e., 7×10^{13} W/cm^2 [8]. One may expect that the electron correlation behavior of strong-field double ionization of Xe could be similar with that of Ar below the recollision threshold, i.e., a dominant back-to-back emission in the laser polarization plane.

Therefore, the knee structure of the integrated yields and the momentum distributions of doubly charged ions cannot reveal the straightforward picture behind the electron dynamics. Thus, it is very necessary to measure electron correlation spectra to identify the ionization mechanism. The measured correlation momentum spectra of Xe from SDI to NSDI are shown in Fig. 2. Here, the momentum of electron "two" was calculated from those of electron "one" and of the $^{134}Xe^{2+}$ ion by the momentum conservation. The correlation momentum spectra reveal the typical sequential double ionization behavior at all laser intensities. The largest electron momentum probability of double ionization is populated around $[P_\parallel(e_1), P_\parallel(e_2)] = (0, 0)$. One can easily understand the correlation spectrum in the SDI regime, i.e., at an intensity of 3×10^{14} W/cm^2, because the two electrons are released sequentially [5]. However, compared with other targets, i.e., He, Ne, and Ar, the electron correlation spectra are much different from other targets in the NSDI regime. Below the recollision threshold, the dominant back-to-back emission phenomenon was observed for Ar [8]. However, the signature of both the side-by-side emission and back-to-back emission essentially disappears for strong-field double ionization of Xe. The correlation momentum spectra of Xe show a sequential feature over a wide of laser intensity, which suggests very different ionization dynamics from that of low-Z atoms.

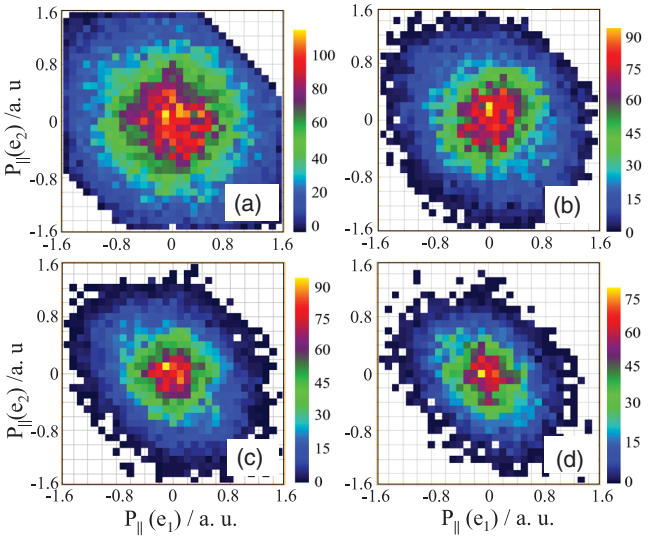

FIG. 2 (color). The measured correlation momentum spectra of double ionization Xe at intensities of (a) 3×10^{14}, (b) 1.6×10^{14}, (c) 7×10^{13}, and (d) 4×10^{13} W/cm^2 (25 fs, 790 nm).

What is the mechanism that introduces the knee structure for strong-field double ionization Xe? Lacking the evident signature of RIDI, one may think that another qualitative picture, i.e., recollision-induced excitation with subsequent ionization (RESI), could explain the Gaussian-like momentum distribution of the doubly charged ion [6]. In the RESI scenario, the recolliding electron with the singly charged ion is assumed to excite the ion near the zero crossing of the laser field. Thereafter, the excited electron then tunnels in one of the subsequent maxima of the laser field and, thus, acquires little drift momentum. The electrons can be emitted either side by side or back to back, thus filling the valley in between the double hump for the momentum distribution of ions. In this spirit, such electron correlation behavior might be expected within the RESI scenario [8].

In order to clarify and highlight the potentially important dynamic mechanism, we further resort to the electron energy spectra of double ionization. Since we have precisely calibrated the laser intensity, we can learn more information from the normalized energy spectra with U_p, as shown in Fig. 3. At an intensity of 3×10^{14} W/cm^2, the

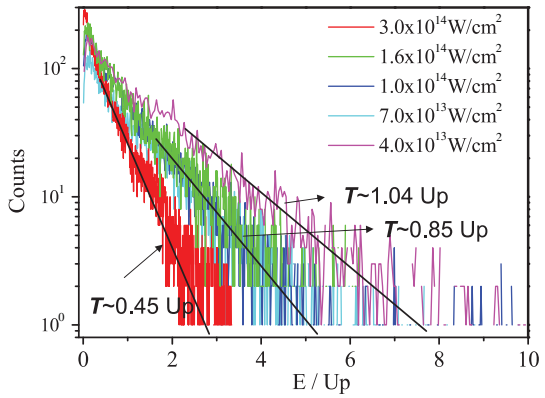

FIG. 3 (color). Intensity dependence of electron energy cutoffs for double ionization Xe in the intensity region of $(0.4–3) \times 10^{14}$ W/cm^2 (25 fs, 790 nm). The solid lines indicate the electron temperature fitted by the Boltzmann distribution (see the text).

electron energy of double ionization has a cutoff around $2.9U_p$ (decreasing about 2 orders), which is close to the maximum drift energy ($\sim 2U_p$) of a free electron gaining from the laser field, indicating that the two electrons are released sequentially and there is not much further interaction between the electrons and ion.

At the lowest intensity, i.e., 4×10^{13} W/cm^2, the maximum recollision energy ($E = 3.17Up \sim 7.6$ eV) is much lower than the second ionization potential (21.3 eV), even less than the potential of the first excitation state $5s5p^6$ of Xe^+ (11.3 eV). The energy cutoff is extended to about $7.8U_p$ at this intensity. In this sense, RESI could explain the electron correlation spectra, but it will fail to explain the electron energy spectra. Fitting the energy spectra with the Boltzmann distribution, one can find that the electrons reveal a temperature in the region of 0.5–$1U_p$. This implies the internal scaling law of high flux photon-atom interactions from the perspective of statistic mechanics.

Obviously, the inner electron is not only a spectator in the recollision process, which can be easily excited by recollisions because there is a larger impact parameter during a recollision for high-Z targets. Multiple rescatterings should be considered for strong-field double ionization at the lowest laser intensity [8]. Multiple rescatterings are not only responsible for producing a much higher kinetic energy photoelectron, but also can facilitate the excitation, because the inner electron is not able to be excited in a single recollision at 4×10^{13} W/cm^2. The double ionization rate of Xe can be enhanced by multiple rescatterings.

In order to include all mechanisms naturally, we have performed a 3D semiclassical two-electron atomic ensemble calculation. This model has been rigorously tested and can work very well for strong-field double ionization of low-Z rare gas atoms [11,24]. Briefly, in the model, one electron is released at the outer edge of the field-suppressed Coulomb barrier through tunneling with a rate given by the ADK theory [23,25]. The bound electron is sampled from a microcanonical distribution. The subsequent evolution of the two electrons with the above initial conditions is governed by Newton's equations of motion: $\frac{d^2 r_i}{dt^2} = -\varepsilon(t) - \nabla_{r_i}(V^i_{ne} + V_{ee})$. Here, index i denotes the two electrons. $V^i_{ne} = -(2/|r_i|)$ and $V_{ee} = 1/|r_1 - r_2|$ are Coulomb interactions between the nucleus and electrons and between two electrons, respectively. The laser field $\varepsilon(t)$ with a cosine waveform has a constant amplitude for the first ten cycles and is turned off with a three-cycle ramp. We consider the recollision-induced excitation tunneling effect in the model. In the calculation, the first and second ionization potentials of the two-electron atom are chosen to match the Xe atom. As seen in Figs. 4(a) and 4(b), the simulations on Xe look more like the electron correlation dynamics of the low-Z rare gas atoms, i.e., He, Ne, and Ar [3–5,8].

Strong-field double ionization has been usually studied by using the heliumlike model atom within the two-active-electron approximation [11,26,27]. However, for those high-Z atoms, the inner electrons will leave a non-negligible influence on the strong-field double ionization. In atoms with many electrons, the outermost electrons are strongly shielded or screened from the nucleus by the inner electrons, known as the shielding or screening effect. The outermost electrons do not feel the complete charge of the nucleus. When the inner electrons are more, the screening effect will be larger. We further improved the above two-electron semiclassical model with the screening potential, $v(r) = -(1/r)[2 + (Z-2)\Omega(r)]$, where $\Omega(r) = [(\eta/\xi)(e^{\xi r} - 1) + 1]^{-1}$ (η and ξ are the potential parameters) [28]. As seen in Figs. 4(c) and 4(d), by considering the shielding effect, the electron correlation momenta are equally distributed in all four quadrants over a wide range of laser intensity and agree well with the measurement. The minimum structure along the coordinate axis is observed in the correlation momentum spectra of theoretical calculation. This is because, in the calculation, we have to stop the evolution of electrons when the laser field switches off to save computer time. The yields of the near-zero-momentum electron will decrease slightly.

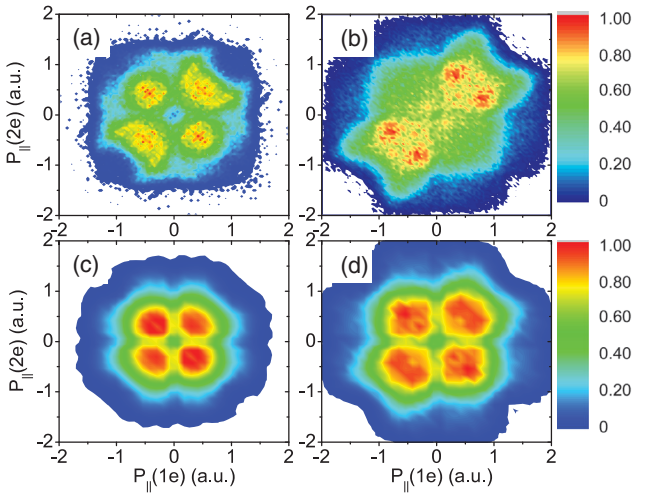

FIG. 4 (color). The calculated correlation momentum spectra of double ionization Xe at intensities of 0.6×10^{14} (a) and 1.1×10^{14} W/cm^2 (b) with the Coulomb potential. The calculated correlation momentum spectra of double ionization Xe at intensity of 0.6×10^{14} (c) and 1.1×10^{14} W/cm^2 (d) using the shielding potential.

In summary, we have comprehensively measured the strong-field double ionization of Xe atoms. Although the curves of the integrated ion yields vs the laser intensity of all rare gas atoms show the general knee structure, the dramatically different electron correlation behavior of strong-field double ionization of Xe atoms was observed, as compared with other targets, i.e., He, Ne, and Ar. The pronounced double-hump structure that was observed in the longitudinal momentum distributions of doubly charged ions of low-Z atomic targets disappears for double ionization of Xe. Lacking the signature of the side-by-side and back-to-back emission, the electron momentum spectra

reveal the remarkable noncorrelation behavior. The fully differential data provide the most direct experimental evidence that the enhanced ionization rate of Xe^{2+} is due to the correlated high-order sequential process (sequential ionization from the excited states) [14,18]. Electron multiple rescatterings lead to high energy photoelectrons at low laser intensities. We have shown that the recollision-induced excitation and the shielding effect are very important for strong-field double ionization of high-Z atoms.

We acknowledge the support by the 973 program (Grants No. 2013CB922403, No. 2013CB834100, and No. 2013CBA01502), the NSFC (Grants No. 11125416, No. 11434002, No. 11121091, No. 11374040, No. 11274051, and No. 11134001), and the Research Foundation for the Returned Overseas Chinese Scholars of State Education Ministry of China.

*lbfu@iapcm.ac.cn
†yunquan.liu@pku.edu.cn

[1] D. N. Fittinghoff, B. Yang, L. F. DiMauro, and K. C. Kulander, Phys. Rev. Lett. **69**, 2642 (1992); B. Walker, L. DiMauro, P. Agostini, K. Schafer, and K. Kulander, Phys. Rev. Lett. **73**, 1227 (1994).
[2] K. Schafer, B. Yang, L. DiMauro, and K. Kulander, Phys. Rev. Lett. **70**, 1599 (1993); P. Corkum, Phys. Rev. Lett. **71**, 1994 (1993).
[3] Th. Weber *et al.*, Phys. Rev. Lett. **84**, 443 (2000); A. Rudenko, V. de Jesus, Th. Ergler, K. Zrost, B. Feuerstein, C. Schröter, R. Moshammer, and J. Ullrich, Phys. Rev. Lett. **99**, 263003 (2007); A. Staudte, C. Ruiz, M. Schöffler, S. Schössler, D. Zeidler, Th. Weber, M. Meckel, D. Villeneuve, P. Corkum, A. Becker, and R. Dörner, Phys. Rev. Lett. **99**, 263002 (2007).
[4] M. Weckenbrock *et al.*, Phys. Rev. Lett. **92**, 213002 (2004); R. Moshammer *et al.*, Phys. Rev. Lett. **84**, 447 (2000); Y. Liu *et al.*Phys. Rev. Lett. **104**, 173002 (2010).
[5] Th. Weber, Th. Weber, H. Giessen, M. Weckenbrock, G. Urbasch, A. Staudte, L. Spielberger, O. Jagutzki, V. Mergel, and M. Vollmer, Nature (London) **405**, 658 (2000).
[6] B. Feuerstein *et al.*, Phys. Rev. Lett. **87**, 043003 (2001); V. L. B. de Jesus, B. Feuerstein, K. Zrost, D. Fischer, A. Rudenko, F. Afaneh, C. D. Schröter, R. Moshammer, and J. Ullrich, J. Phys. B **37**, L161 (2004).
[7] W. Becker, X. Liu, P. Jo Ho, and J. H. Eberly, Rev. Mod. Phys. **84**, 1011 (2012).
[8] Y. Liu, S. Tschuch, A. Rudenko, M. Dürr, M. Siegel, U. Morgner, R. Moshammer, and J. Ullrich, Phys. Rev. Lett. **101**, 053001 (2008).
[9] E. Eremina *et al.*, J. Phys. B **36**, 3269 (2003).
[10] S. L. Haan, Z. S. Smith, K. N. Shomsky, and P. W. Plantinga, J. Phys. B **41**, 211002 (2008).
[11] D.-F. Ye and J. Liu, Phys. Rev. A **81**, 043402 (2010).
[12] T. Shaaran and C. Figueira de Morisson Faria, J. Mod. Opt. **57**, 984 (2010).
[13] A. L'Huillier, L. A. Lompre, G. Mainfray, and C. Manus, Phys. Rev. A **27**, 2503 (1983).
[14] D. Charalambidis, P. Lambropoulos, H. Schröder, O. Faucher, H. Xu, M. Wagner, and C. Fotakis, Phys. Rev. A **50**, R2822 (1994).
[15] A. Talebpour, C.-Y. Chien, Y. Liang, S. Larochelle, and S. L. Chin, J. Phys. B **30**, 1721 (1997).
[16] R. Wiehle and B. Witzel, Phys. Rev. Lett. **89**, 223002 (2002).
[17] J. L. Chaloupka, J. Rudati, R. Lafon, P. Agostini, K. Kulander, and L. DiMauro, Phys. Rev. Lett. **90**, 033002 (2003).
[18] J. Rudati, J. L. Chaloupka, P. Agostini, K. C. Kulander, and L. F. DiMauro, Phys. Rev. Lett. **92**, 203001 (2004).
[19] P. Kaminski, R. Wiehle, W. Kamke, H. Helm, and B. Witzel, Phys. Rev. A **73**, 013413 (2006).
[20] G. Gingras, A. Tripathi, and B. Witzel, Phys. Rev. Lett. **103**, 173001 (2009).
[21] J. Ullrich, R. Moshammer, A. Dorn, R. Dörner, L. Ph. H. Schmidt, and H. Schmidt-Böcking, Rep. Prog. Phys. **66**, 1463 (2003).
[22] B. Feuerstein, R. Moshammer, and J. Ullrich, J. Phys. B **33**, L823 (2000).
[23] M. V. Ammosov, N. B. Delone, and V. P. Krainov, Zh. Eksp. Teor. Fiz. **91**, 2008 (1986) [Sov. Phys. JETP **64**, 1191 (1986)].
[24] D. F. Ye, X. Liu, and J. Liu, Phys. Rev. Lett. **101**, 233003 (2008); Y. Liu, L. Fu, D. Ye, J. Liu, M. Li, C. Wu, Q. Gong, R. Moshammer, and J. Ullrich, Phys. Rev. Lett. **112**, 013003 (2014).
[25] N. B. Delone and V. P. Krainov, J. Opt. Soc. Am. B **8**, 1207 (1991).
[26] J. Ho Phay, R. Panfili, S. L. Haan, and J. H. Eberly, Phys. Rev. Lett. **94**, 093002 (2005); S. L. Haan, L. Breen, A. Karim, and J. H. Eberly, Phys. Rev. Lett. **97**, 103008 (2006).
[27] J. S. Parker, B. Doherty, K. Taylor, K. Schultz, C. Blaga, and L. DiMauro, Phys. Rev. Lett. **96**, 133001 (2006).
[28] R. H. Garvey, C. H. Jackman, and A. E. S. Green, Phys. Rev. A **12**, 1144 (1975).